



**AFOSR MURI in FUNDAMENTAL
PROCESSES IN HIGH-TEMPERATURE
HYPERSONIC FLOWS**

July 15, 2013,

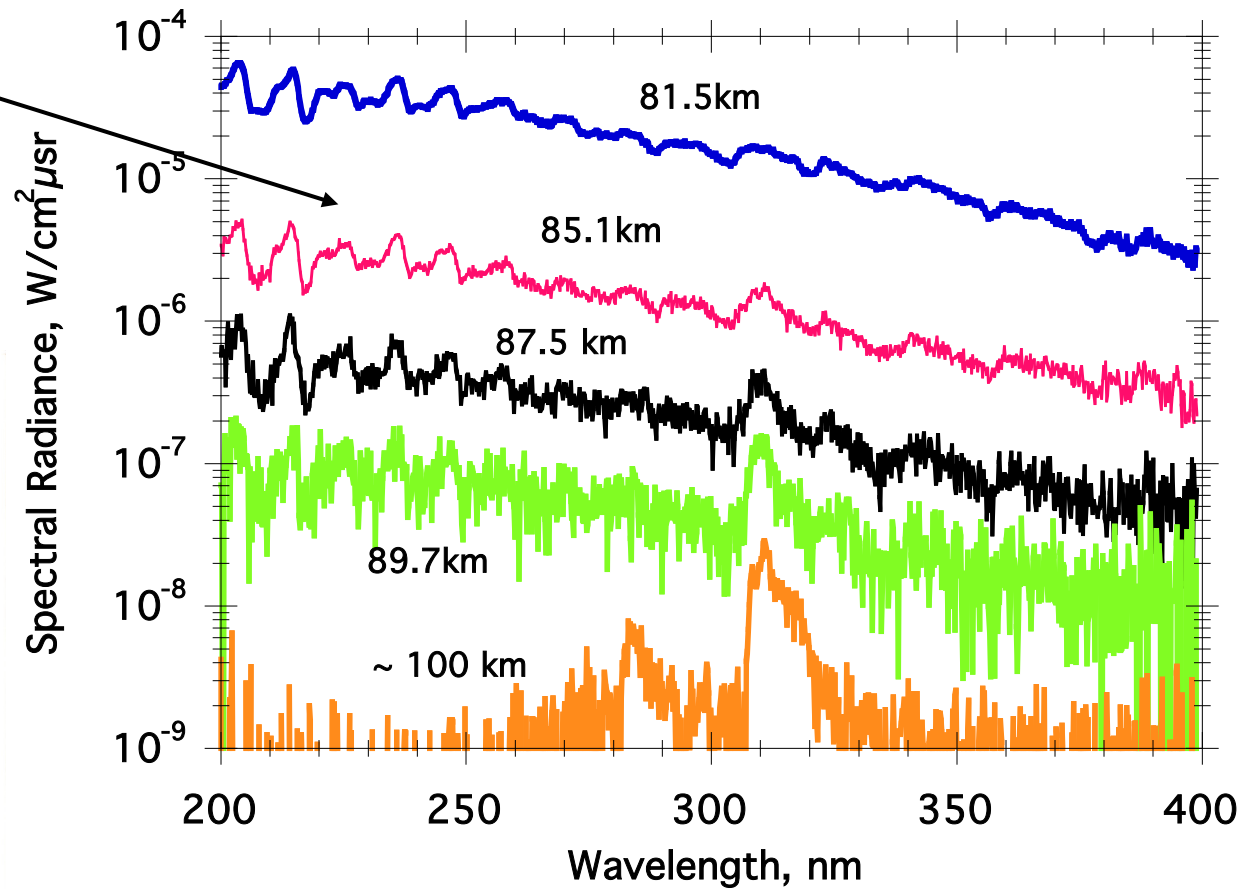
**AFOSR – MURI Review
Arlington, VA**

***Design and Analyses of
Nonequilibrium Gas Kinetic
Experiments***

**Zheng Li, Tong Zhu, Neal Parsons, and
Deborah A. Levin**

Expansion of High-Altitude Portion of BSUV2 Trajectory

NO spectral radiation



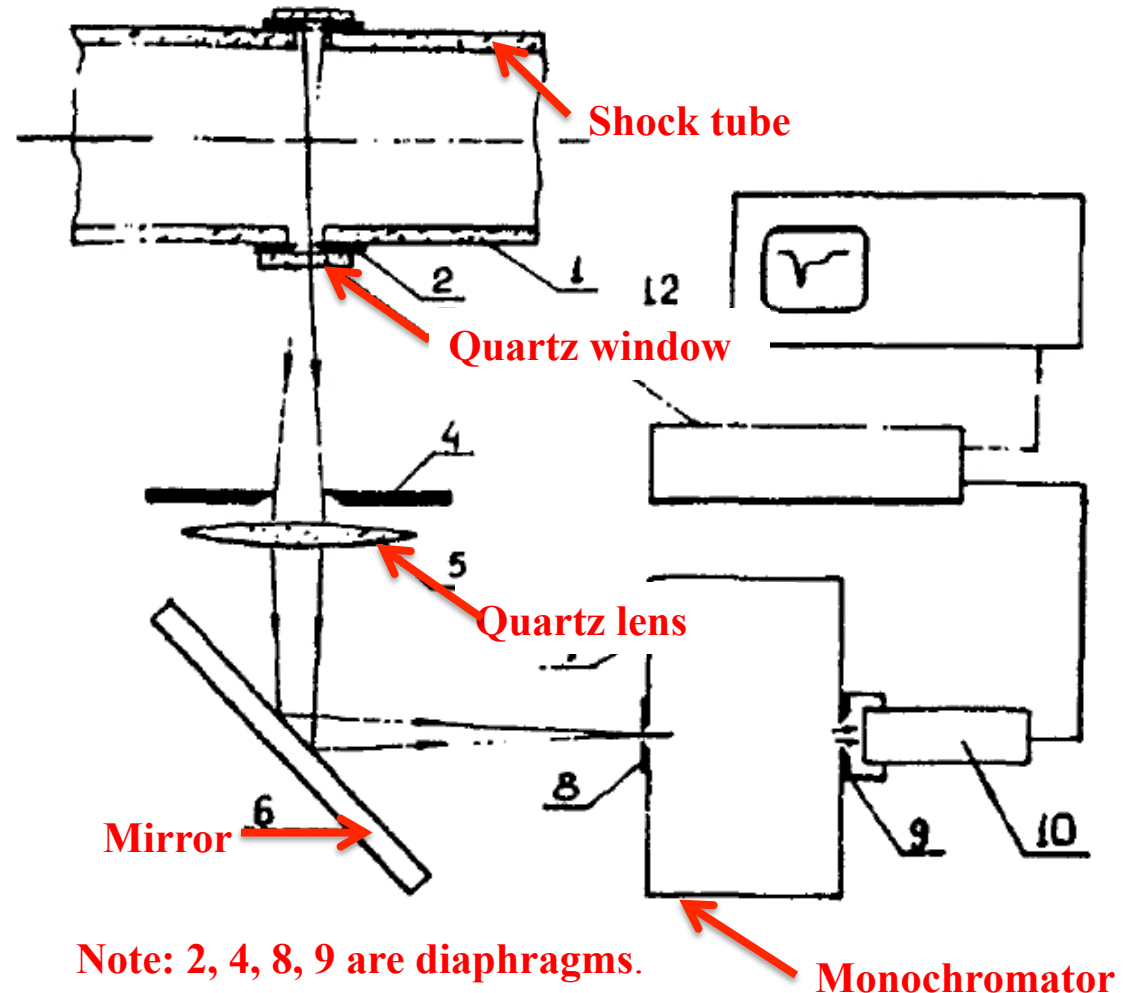
Direct Simulation Monte Carlo



1. DSMC follows the motions of many virtual particles on a grid over a series of time steps, tracking their collisions.
2. Particle-surface collisions are calculated.
3. Reactions and changes in internal energies and velocities of the components are also tracked.
4. Particles are indexed within cells.
5. Particle collision outcomes (i.e., relaxation and chemistry) are calculated using Monte Carlo techniques.
6. Post-collision velocities are determined, observing conservation of energy and momentum.
7. Provides multi-scale approach to modeling thermochemical nonequilibrium in hypersonic shock layers.

Experiment by Gorelov *et al.**

- Measurements taken in an electrically arc-driven shock tube.
- The length of the low-pressure-driven channel is about 5 m with an inner diameter of 57 mm.
- The optical system is shown to the right:
 - spatial resolution of 0.1mm.
 - temporal resolution of about 0.1 μ s.

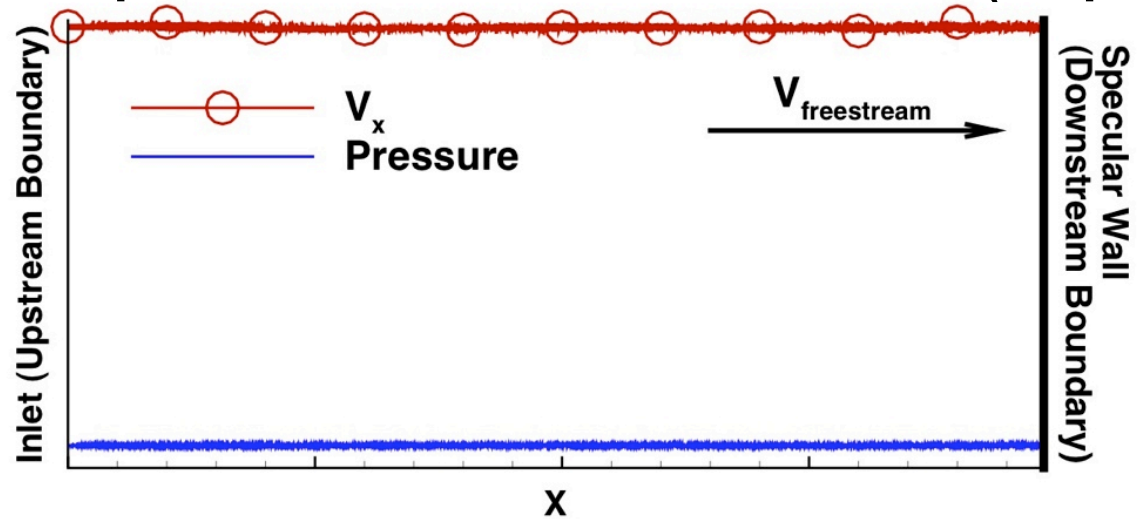


*V. Gorelov, M. Gladyshev, A. Kireev, I. Yegorov, Yu. Plastinin, and G. Karabadzhak, "Experimental and Numerical Study of Nonequilibrium Ultraviolet NO and N₂⁺ Emission in Shock Layer," JTHT, Vol. 12, No. 2, April – June 1998

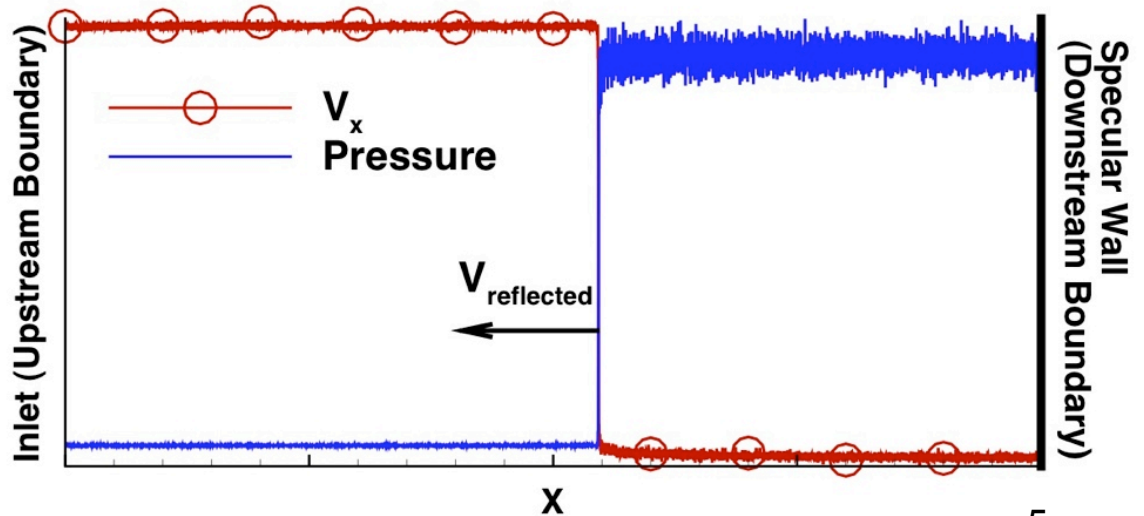
Generation of a 1-D Reflected Shock (1/3)*

Setup of the Computation Domain and Initialization (Step 1)

Initial condition



Propagation of reflected shock



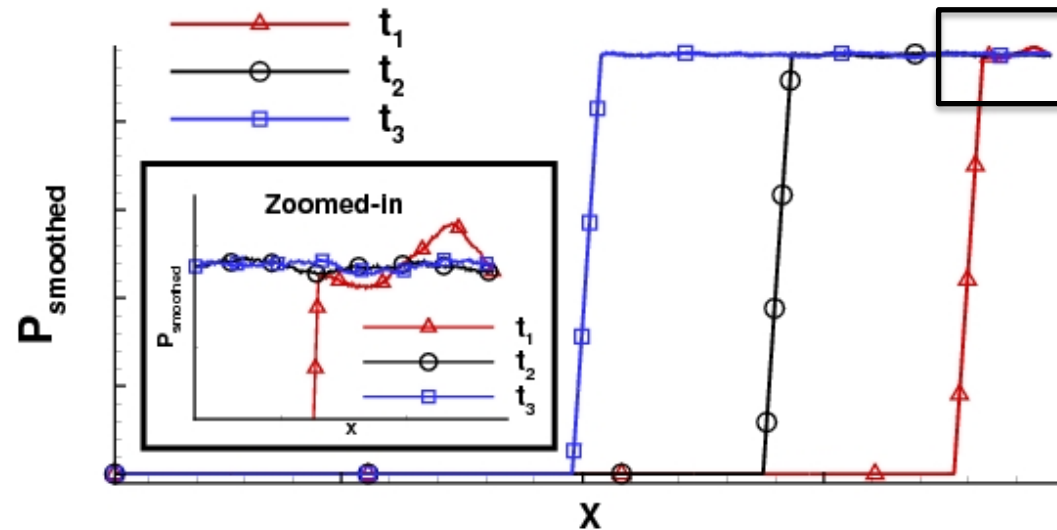
*Strand, J. S., *Statistical Methods for the Analysis of DSMC Simulation of Hypersonic Shocks*, Ph.D. thesis, The University of Texas at Austin, 2012



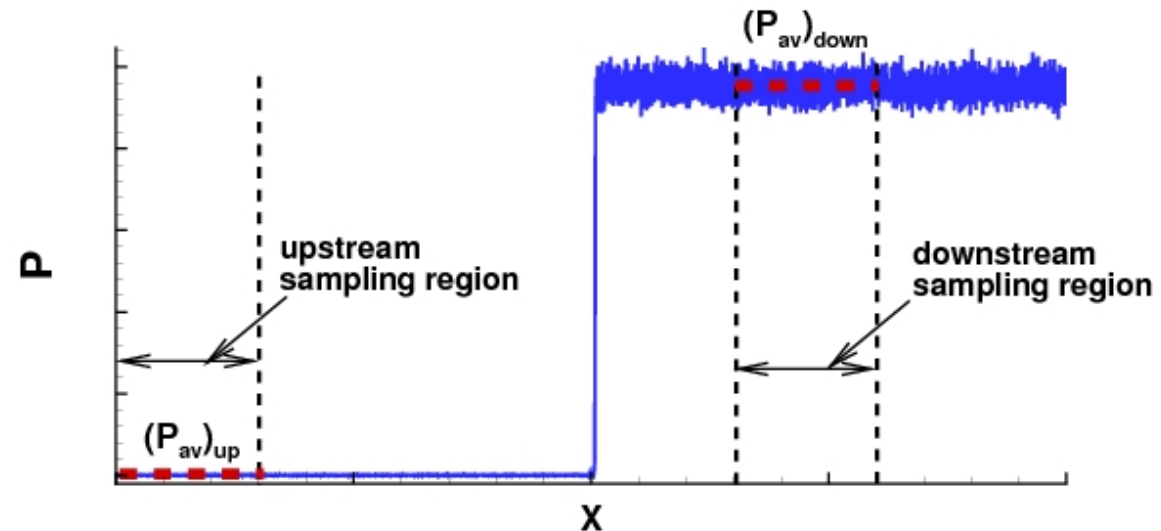
Generation of a 1-D Reflected Shock (2/3)

Pressure Monitoring and Determination of Downstream Conditions (Step 2)

Observation of the box-car smoothed pressures suggests that after t_3 , the flow can be sampled.



Sampling regions

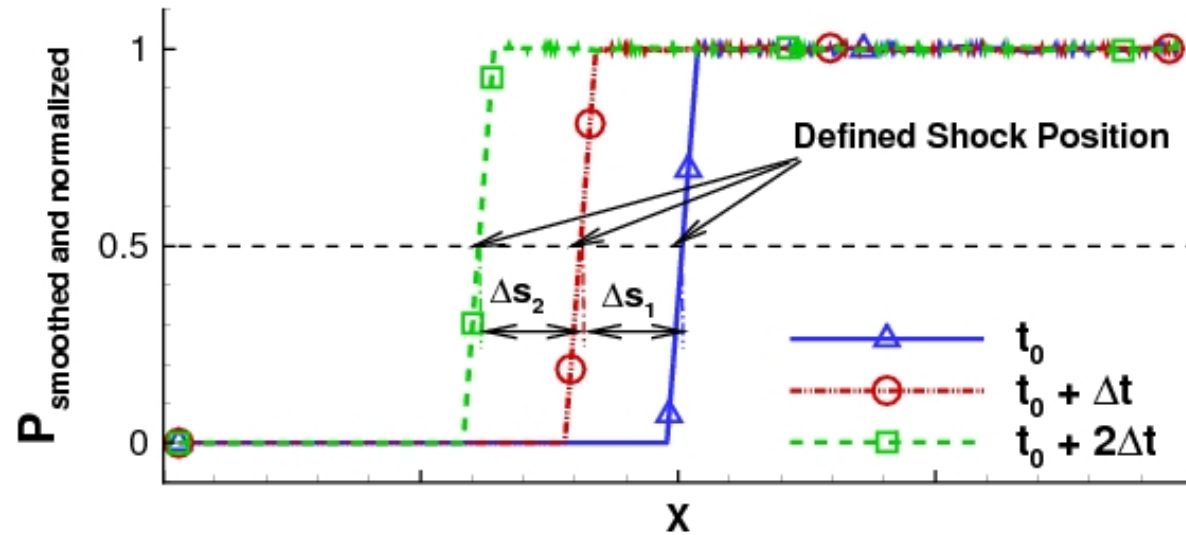




Generation of a 1-D Reflected Shock (3/3)

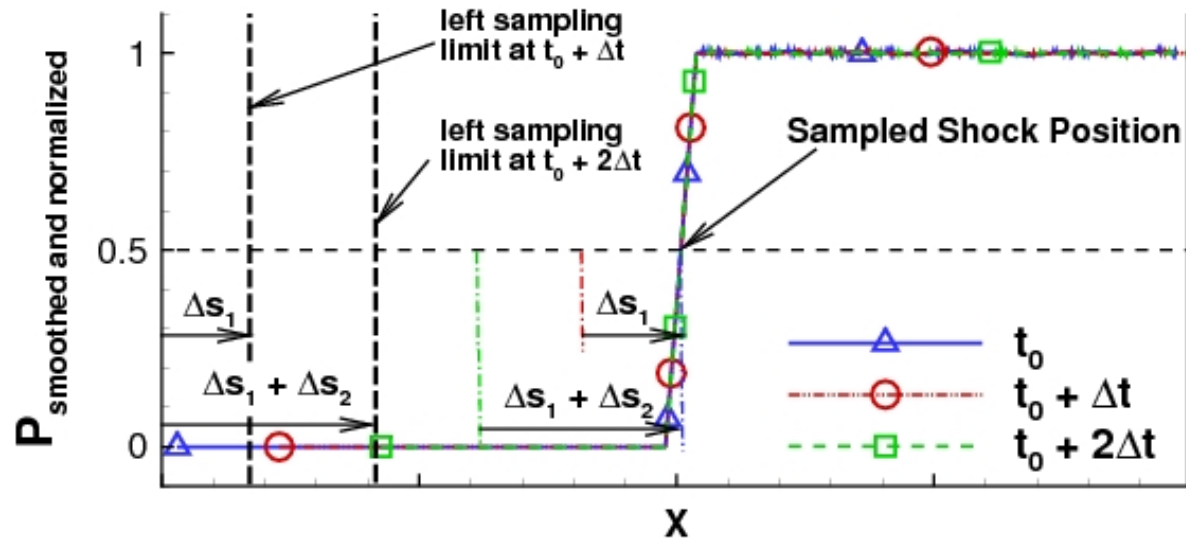
Shock Speed Monitoring and Equivalent “Moving-window” Sampling Approach (Step 3)

The original “moving-window” sampling



$$P_{norm} = \frac{P - (P_{av})_{up}}{(P_{av})_{down} - (P_{av})_{up}}$$

Equivalent approach



Conditions for Reflected Shock Cases and Flow Over a Cylinder

- Free stream parameters for the two types of calculations are summarized in the table to the right.

Parameter	Shock Tube for Air	Cubic Cylinder Test *	
		Run 5	Run 6
Streamwise Velocity (m/s)	4000, 5000, 6000, 7000, 8000, 9000	4840	5380
Temperature (K)	300	261	215
Number Density (Molecule/m ³)	3.2188×10 ²¹	2.69×10 ²¹	1.22×10 ²¹
N ₂ mole fraction(%)	79	79	79
O ₂ mole fraction(%)	21	21	21
Mean free path (m)	0.450×10 ⁻³	0.525×10 ⁻³	1.112×10 ⁻³

- In reflected shock cases, the **effective upstream velocities, V_{eff}** , are obtained by adding the reflected shock speed to the freestream speed: $V_{eff} = V_{\infty} + V_{refl}$ as shown in the table to the right.

$V_{upstream}$ (m/s)	$V_{effective}$ (m/s)	$Ma_{effective}$
4000	4427.8	12.73
5000	5447.73	15.66
6000	6430.49	18.48
7000	7427.13	21.35
8000	8452.53	24.29
9000	9853.85	28.32

* Correspond to the Runs 5 and 6 in the paper “Emission Measurements from High Enthalpy Flow on a Cylinder in the LENS-XX Hypervelocity Expansion Tunnel,” Parker, R., Holden, M., DesJardin, P., Weisberger, J., and Levin, D., AIAA paper 2013-1058, 2013



Models used in DSMC Simulations

- VHS collision model and the Larsen-Borgnakke (LB) internal energy relaxation model were used.
- The total collision energy (TCE) model of Bird was used for the chemical reactions listed below:

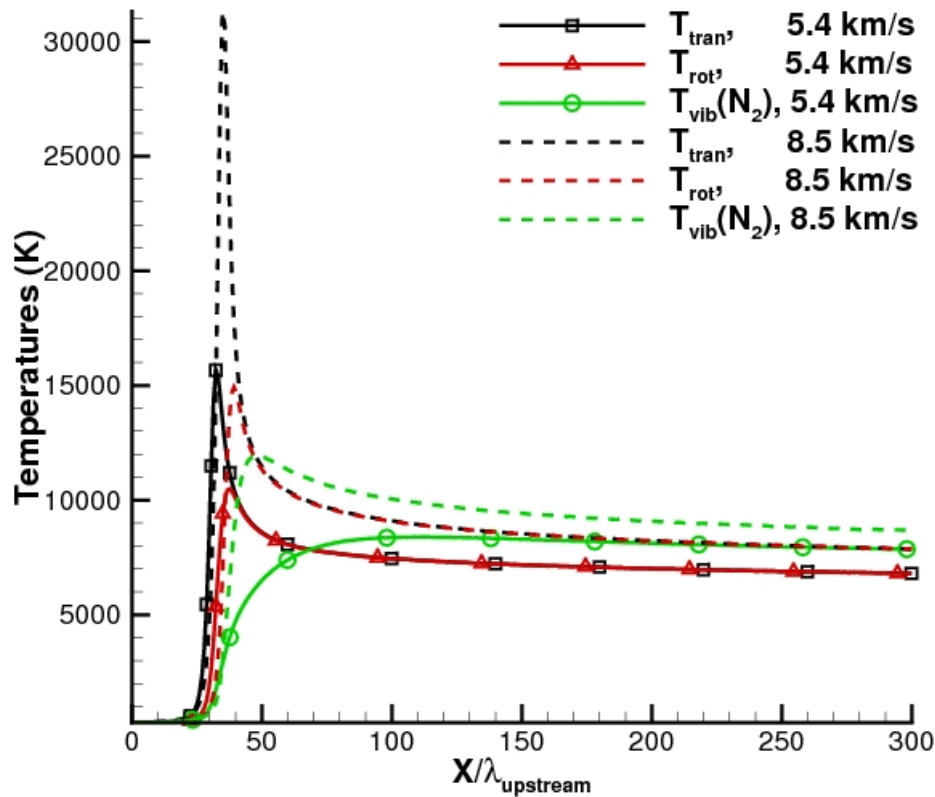
Reaction*	A, m ³ /s	n	E _a , × 10 ⁻¹⁹ J
N ₂ +N ₂ to N ₂ +N+N	1.16×10 ⁻⁸	-1.6	15.63
M+N ₂ to M+N+N	4.98×10 ⁻⁸	-1.6	15.63
M+O ₂ to M+O+O	3.32×10 ⁻⁹	-1.5	8.214
M+NO to M+N+O	8.30×10 ⁻¹⁵	0	10.42
N ₂ +O to NO+N	9.45×10 ⁻¹⁸	0.42	5.928
O ₂ +N to NO+O	4.13×10 ⁻²¹	1.18	0.553
NO+N to N ₂ +O	2.02×10 ⁻¹⁷	0.1	0
NO+O to O ₂ +N	1.40×10 ⁻¹⁷	0	2.653

* Reaction rate coefficient, $k_r = A T^n \exp(-E_a/kT)$.

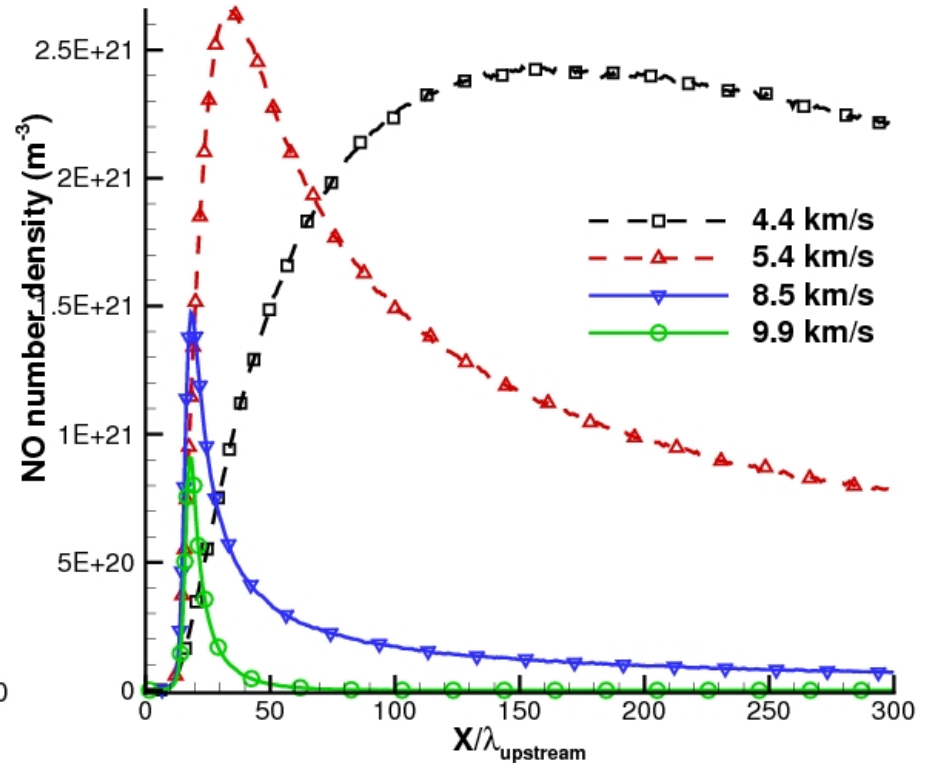
1-D Reflected Shock Cases: Temperatures and NO Number Densities

$$V_\infty = 4\sim 9\text{ km/s}, n_\infty = 3.22 \times 10^{21}/\text{m}^3, T_\infty = 300\text{ K}$$

Temperatures



NO Number Densities

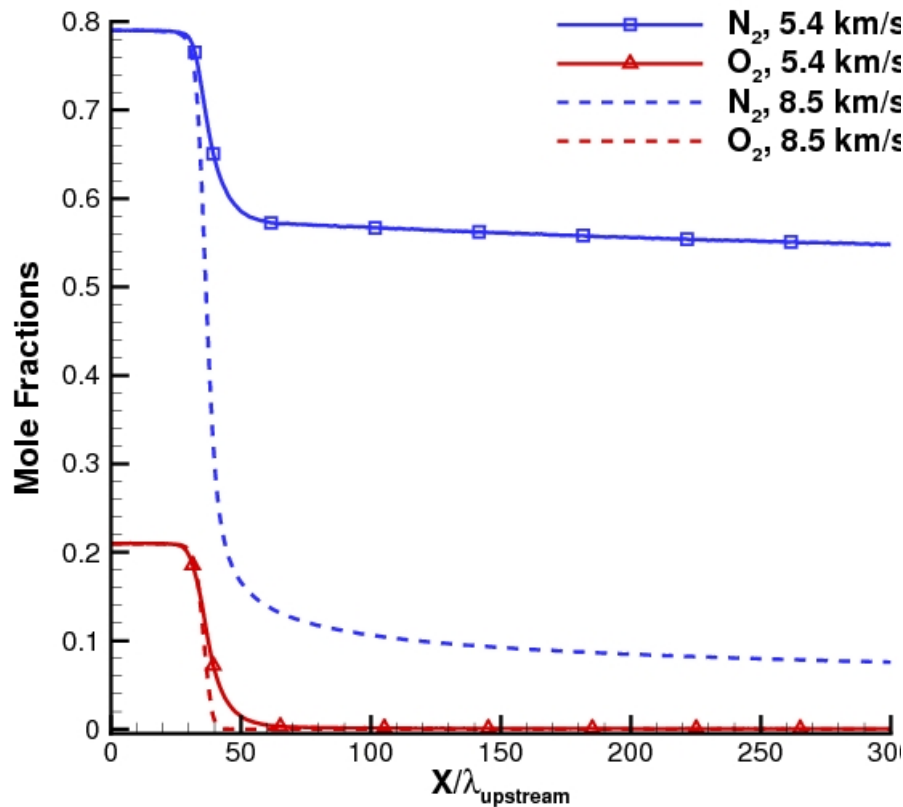


- As the shock speed increases, the peak value for NO number density first increases then decreases.

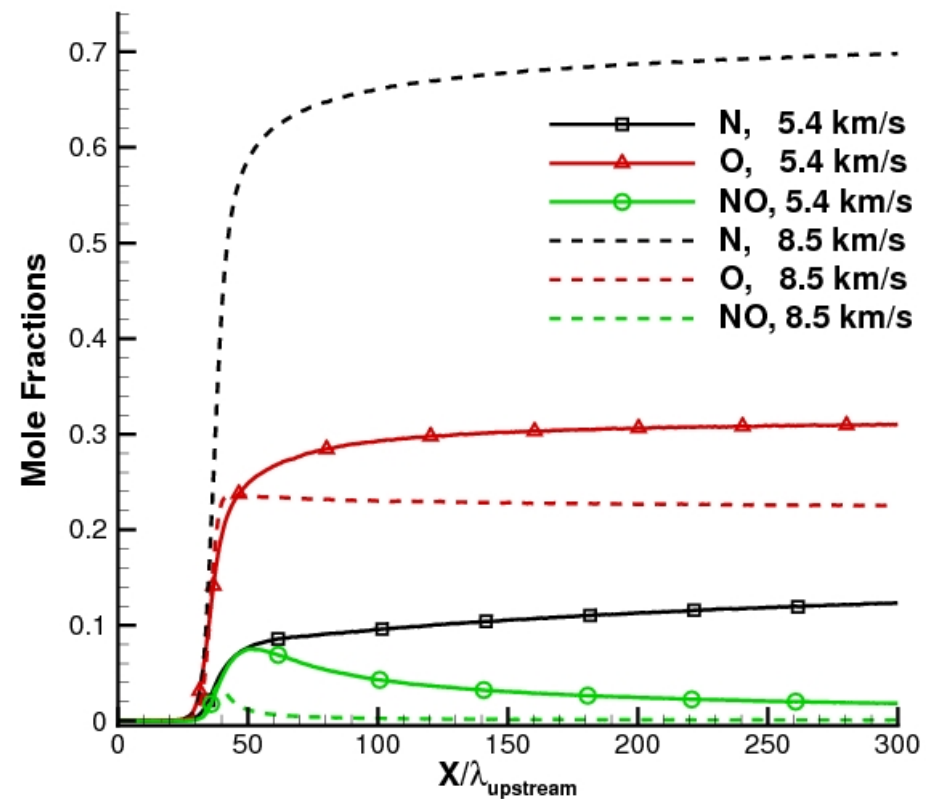
1-D Reflected Shock Cases: Species Mole Fractions

$V_\infty = 4\sim 9\text{ km/s}$, $n_\infty = 3.22 \times 10^{21}/\text{m}^3$, $T_\infty = 300\text{ K}$

N_2 and O_2



N, O and NO

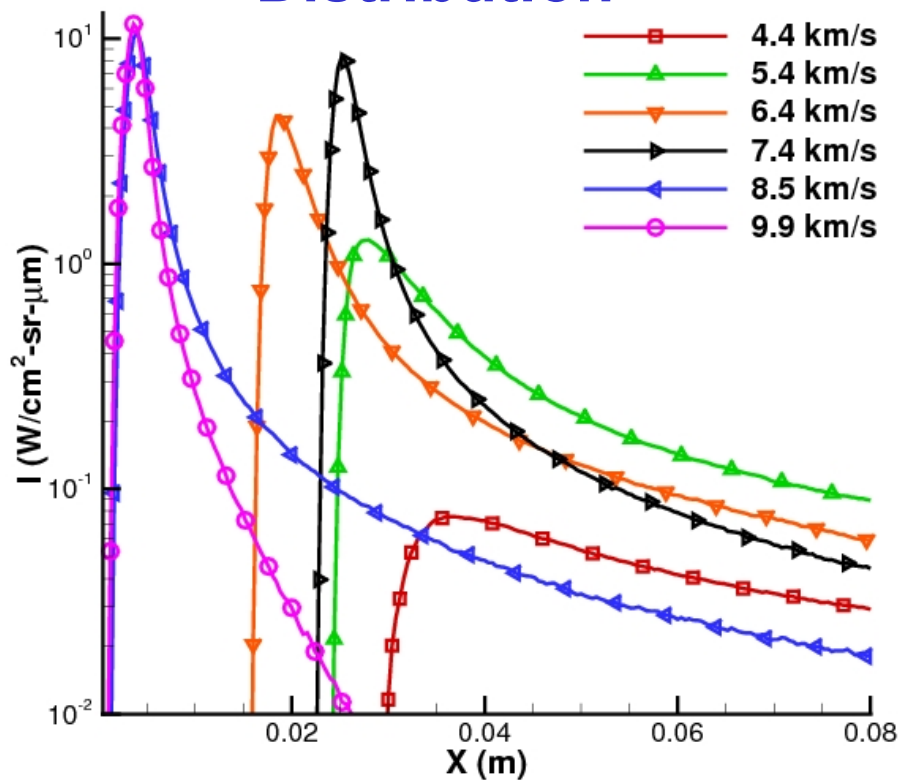


- O_2 is almost fully dissociated while N_2 requires more energy or higher shock speeds to be dissociated.

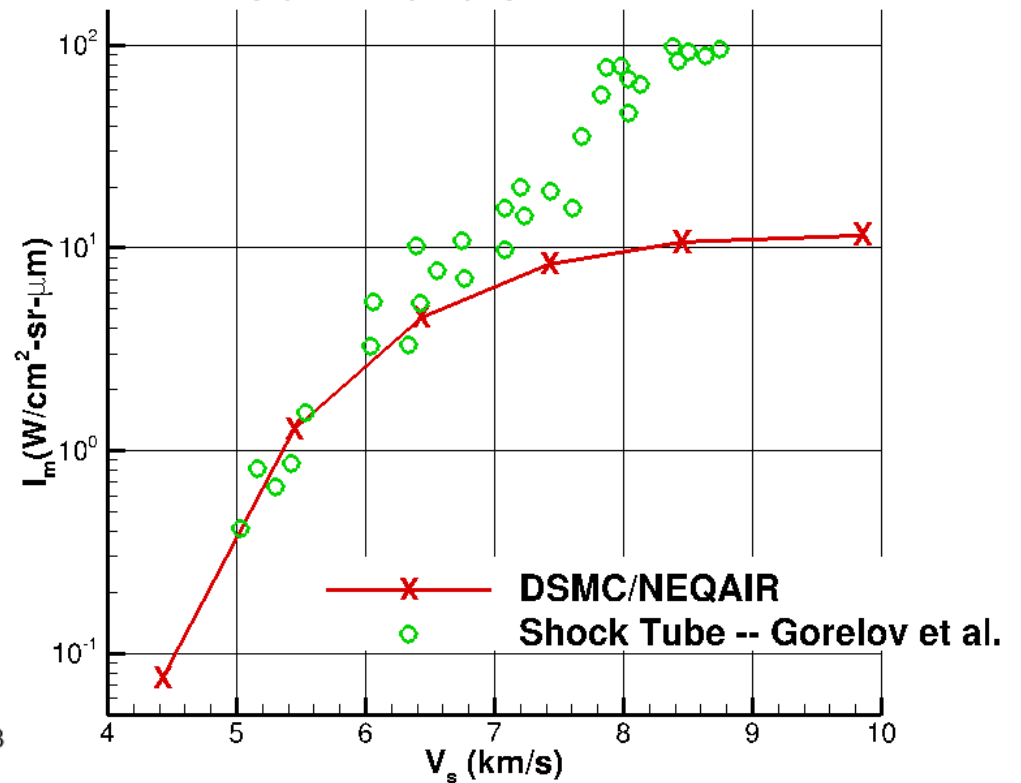
1-D Reflected Shock Cases: Radiation Intensity ($\lambda = 235 \pm 7$ nm)

$V_\infty = 4\sim 9$ km/s, $n_\infty = 3.22 \times 10^{21}/\text{m}^3$, $T_\infty = 300$ K

Distribution



Peak value

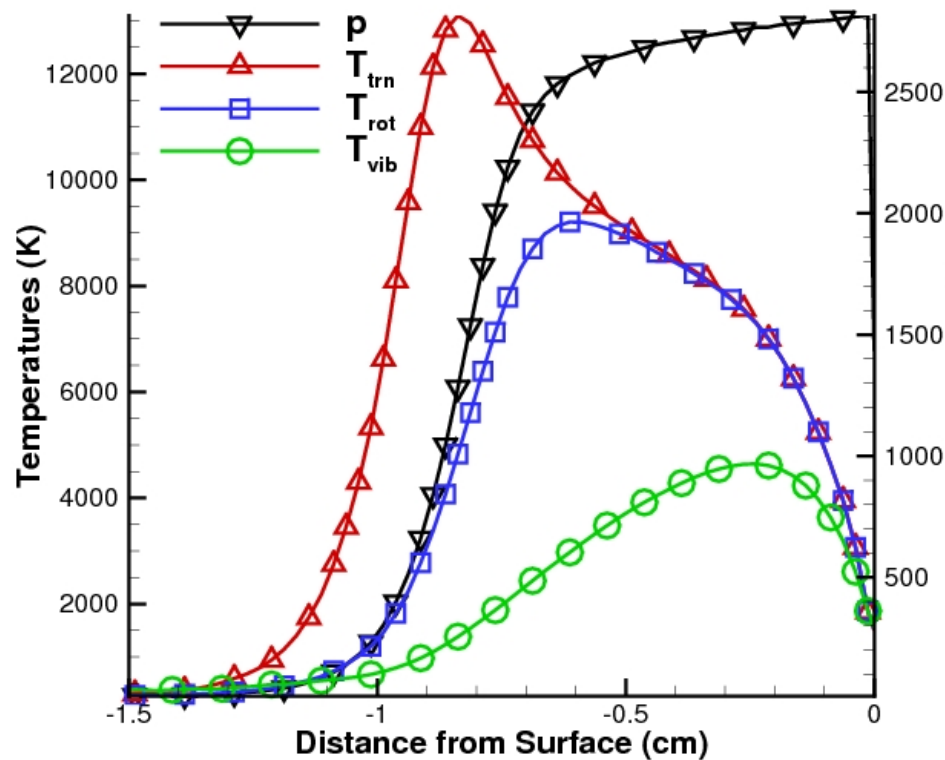


- Calculations are in good agreement with experiment for shock speeds < 7 km/s, but, is lower than the experiment for shock speeds > 7 km/s. 12

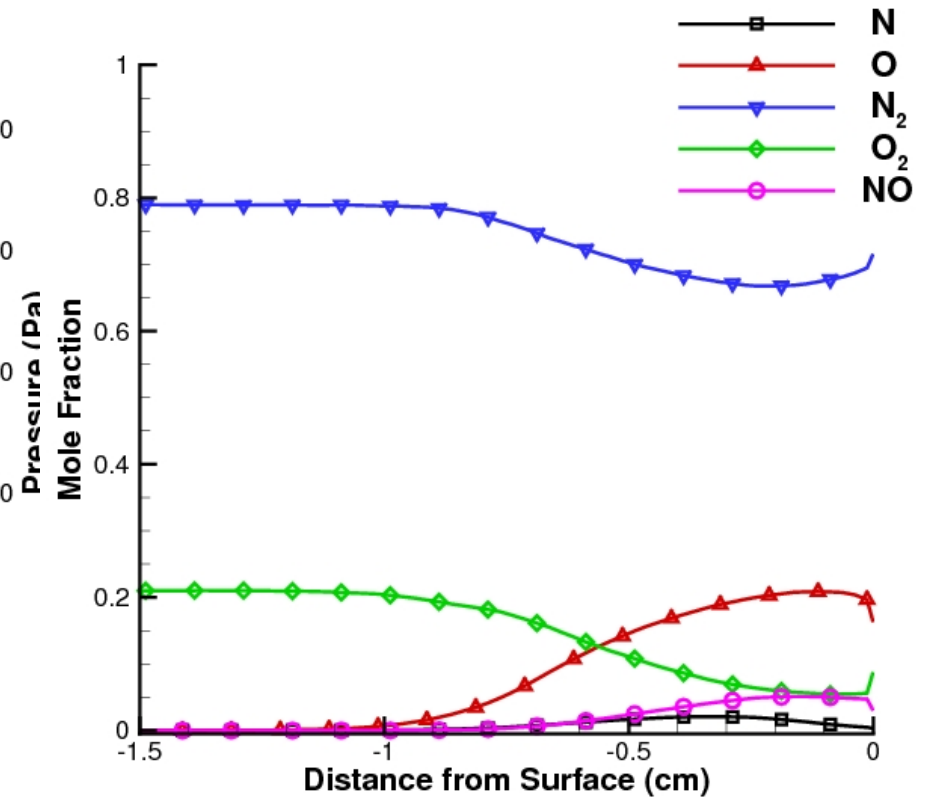
Flow Over a Cylinder - Run 5 LENS-XX

(66km altitude, $V_\infty = 4.84\text{km/s}$, $n_\infty = 2.69 \times 10^{21}/\text{m}^3$, $T_\infty = 261\text{K}$)

Temperature and Pressure



Mole Fractions

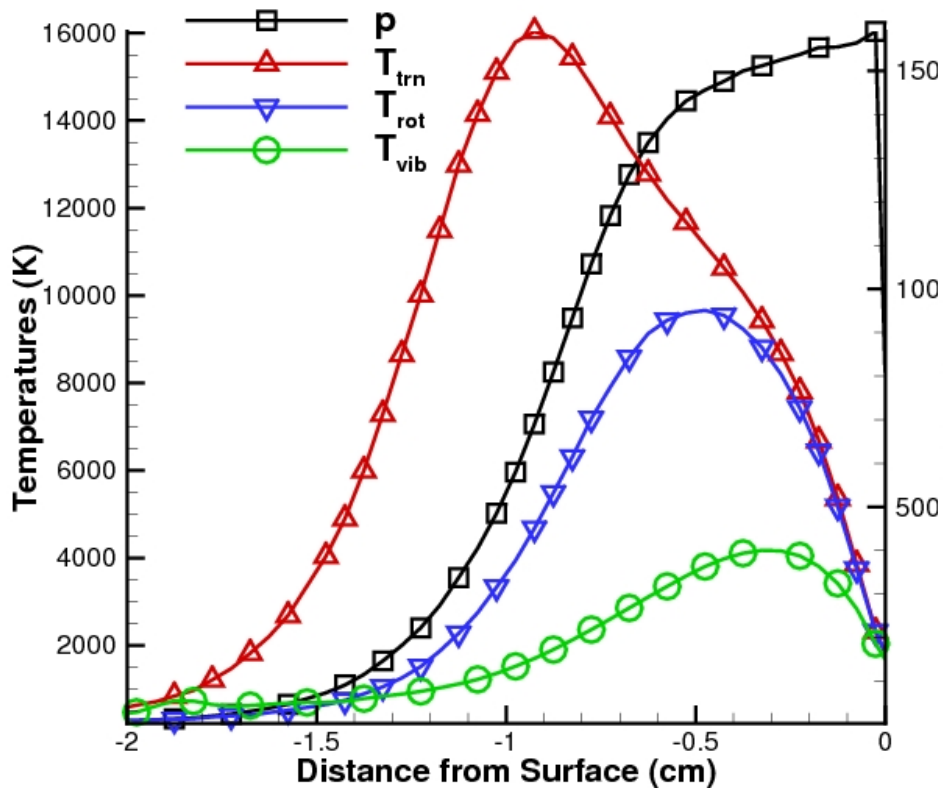


- Compared with CFD calculations by Parker *et al.*, the DSMC shock standoff distance and shock thickness are larger.
- Both the maximum translational and rotational temperatures are higher than the CFD results by about 2000 K.

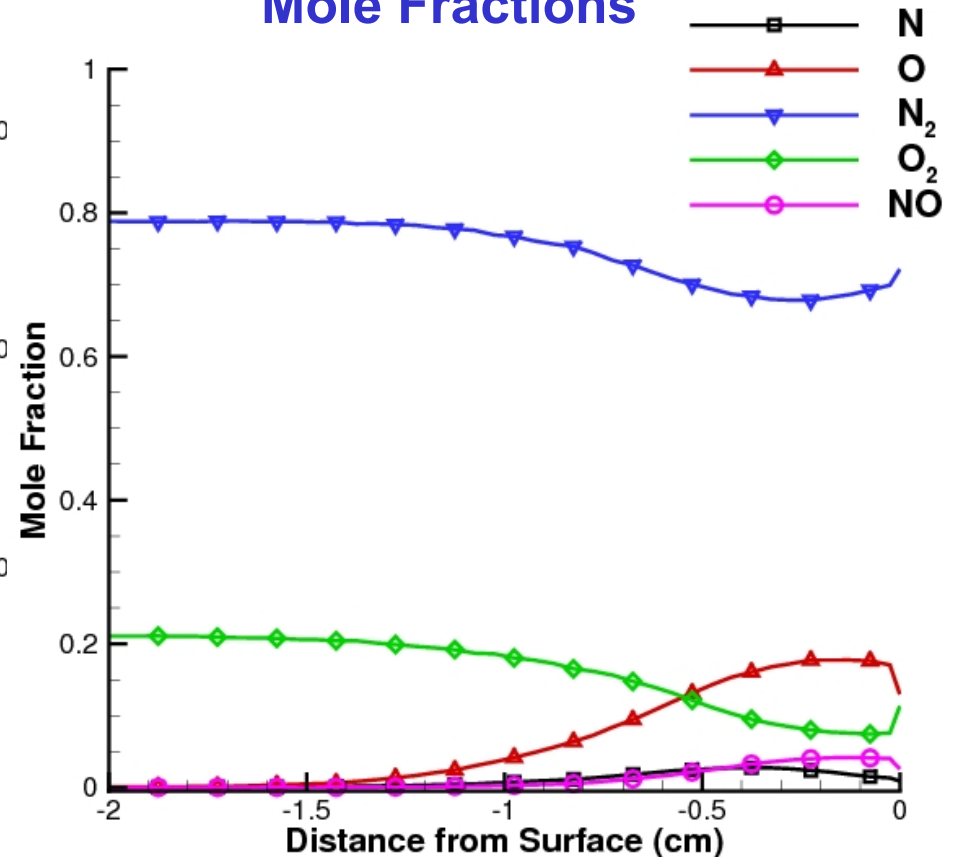
Flow Over a Cylinder - Run 6 LENS-XX

(71.7km altitude, $V_\infty = 5.38\text{km/s}$, $n_\infty = 1.22 \times 10^{21}/\text{m}^3$, $T_\infty = 215\text{K}$)

Temperatures and pressures



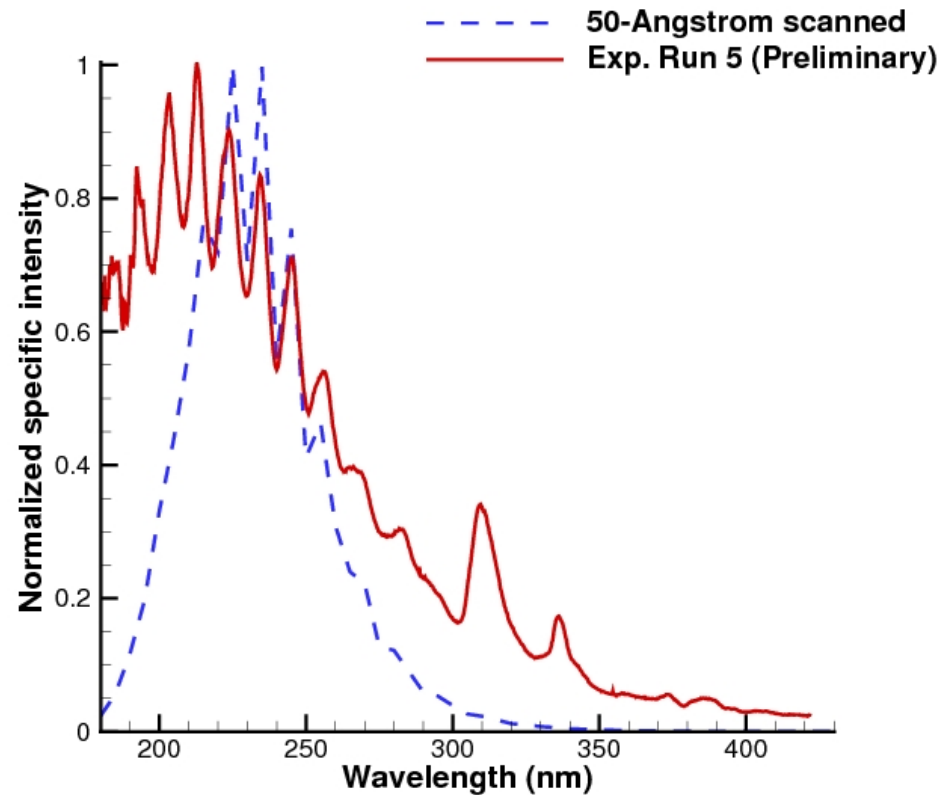
Mole Fractions



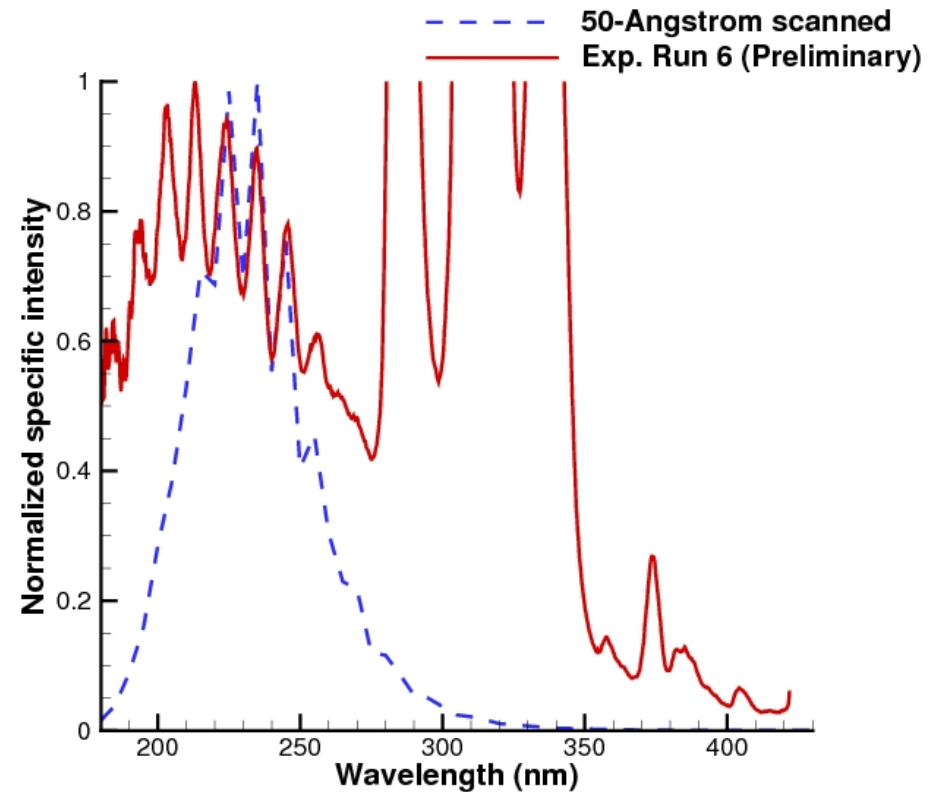
- In this case, the maximum translational and rotational temperatures are higher than the CFD results by about 3000K.

Flow over a Cylinder Runs 5 and 6: Self-normalized Specific Intensities

Run 5



Run 6



The shapes of the calculated scanned specific intensity profiles are partially in agreement with those of experimentally measured data.

Summary of Experimental Modeling & Future Work

- For the unsteady one-dimensional reflected shock simulation, calculated radiation in good agreement with experiment for shock speeds $< 7\text{km/s}$ but is lower than the experiment for shock speeds $> 7\text{km/s}$.
- For the steady flow over a cylinder simulations, the shapes of the calculated scanned specific intensity profiles are sort of in agreement with those of experiments, but, magnitudes $\sim 1\text{-}2$ orders higher - needs to be studied further.
- Future work will include:
 - Inclusion of ionization model and associated electron-impact processes,
 - Radiation from other band systems and also from N_2^+ ,
 - Inclusion of FHO-QCT model with more accurate collision and reaction cross sections from MD/QCT simulations.

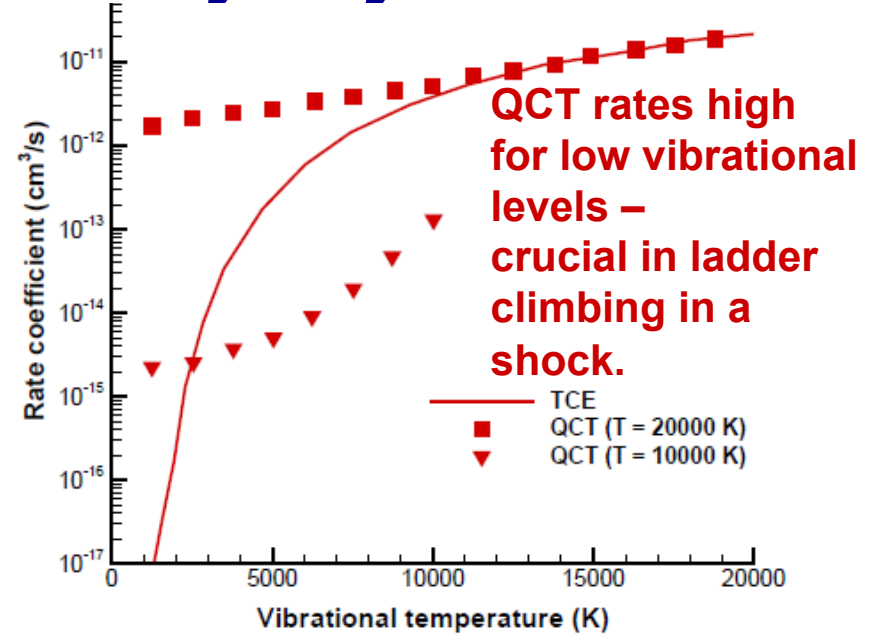
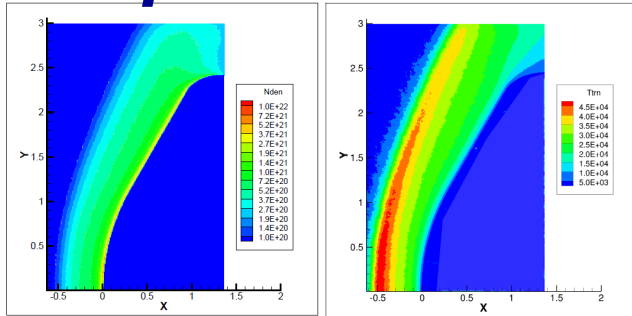


Objectives and Approach of Thermochemical Modelling

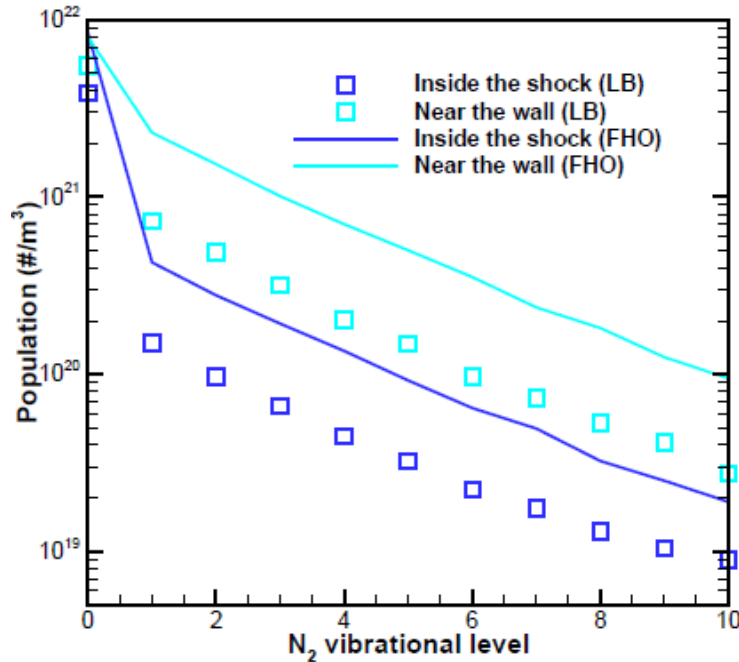
- **The transitions between the vibrationally excited states of the N_2 , its dissociation, and formation of NO from different N_2 vibrational excited states are modeled.**
- **Collisions that cause translational to vibrational energy exchange with better representation of physics have been studied:**
 - Discrete Larson-Bernakke (baseline),
 - Schwartz-Slawsky-Herzfeld (SSH),
 - Forced Harmonic Oscillator (FHO).
- **The chemistry models include: (1) TCE, (2) QCT - Bose, and (3) QCT - Jaffe and Magin (N_2 dissociation):**
 - Original 10,000 ro-vibrational energy levels of N_2 ground state → coarsened to 46 vibrational levels x 10 bins of $E_{QCT} = E_{trns} + E_{rot}$
 - σ_{QCT} based on assumption of $E_{rot} = E_{trans}$
- **Collaborate with D. Truhlar, S. Doraiswamy and G. Candler to use new N3 and N4 potential energy surfaces.**



N₂/N Flow over a Blunt Body - Importance of High-Fidelity Physical Models

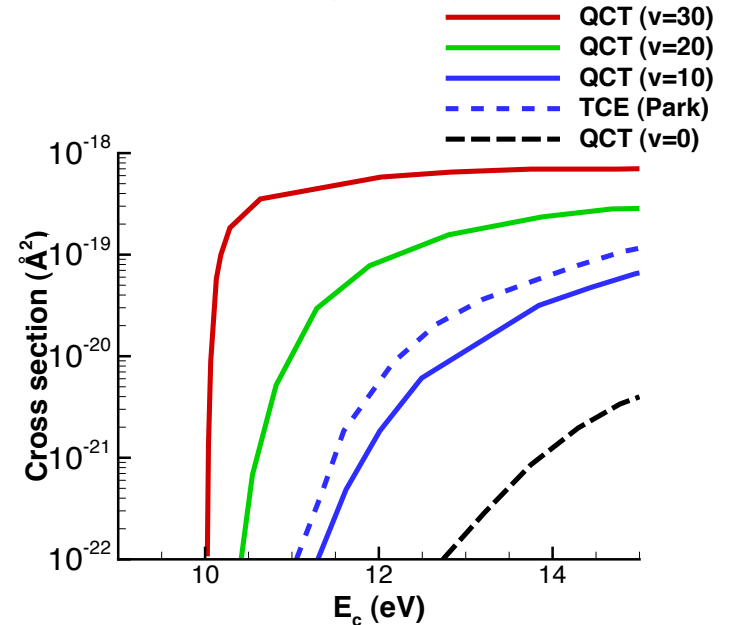


Nonequilibrium Vibrational Distributions – T-V Relaxation



QCT has > degree of dissociation at low vibrational levels

- FHO V-T > LB rates: gives higher vibrational populations and temperatures
- Shock width reduced using FHO model ~ 15% difference



Development of New Rotational Relaxation Model for N₂+N Collisions

Phenomenological Parker T-R relaxation model

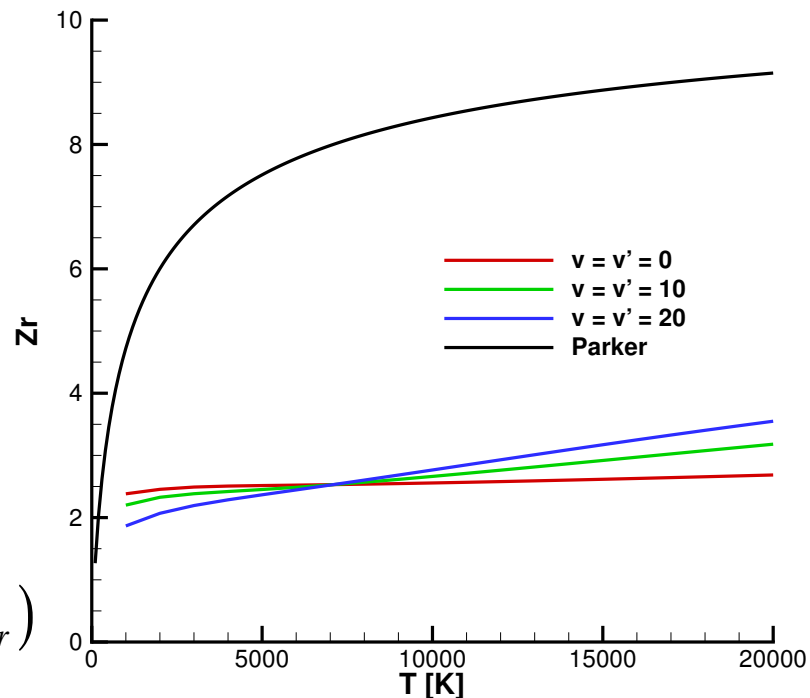
$$Z_r^P = \frac{\zeta_t}{\zeta_t + \zeta_r} f(T, T^* = 91K, Z_r^\infty = 18.5)$$

MD/QCT Approach

$$Z_{r,eff} = \frac{\sigma_{el}(T) + \sigma_r(T)}{\sigma_r(T)}$$

$$\sigma_r(T) = Q_{tr}^{-1} \sum_{E_{tr}=E_{tr,min}}^{E_{tr}=E_{tr,max}} \Delta E_{tr} \exp\left(-E_{tr}/kT\right) \sigma_r(T, E_{tr})$$

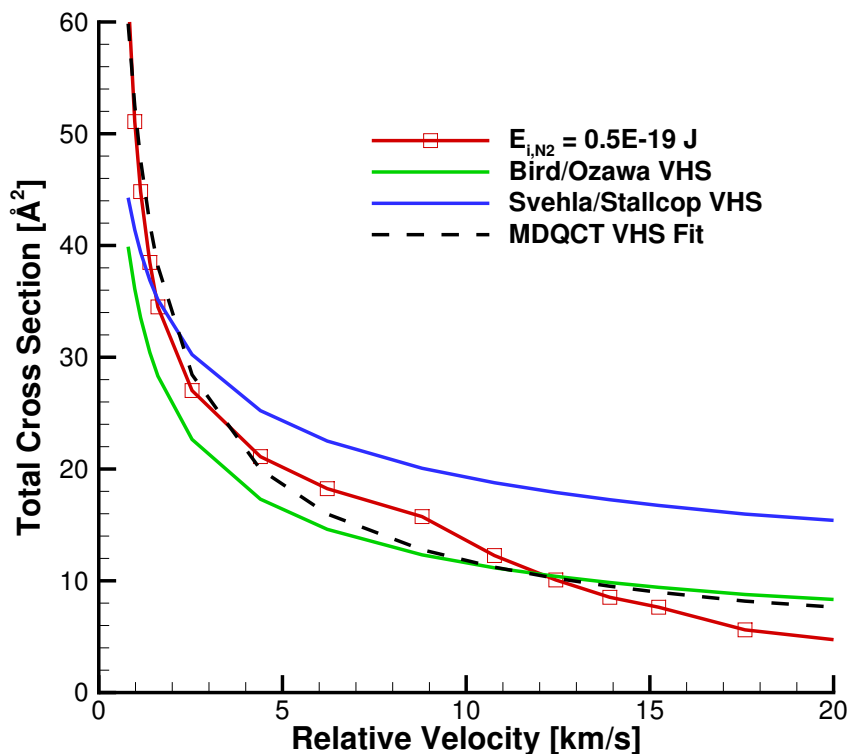
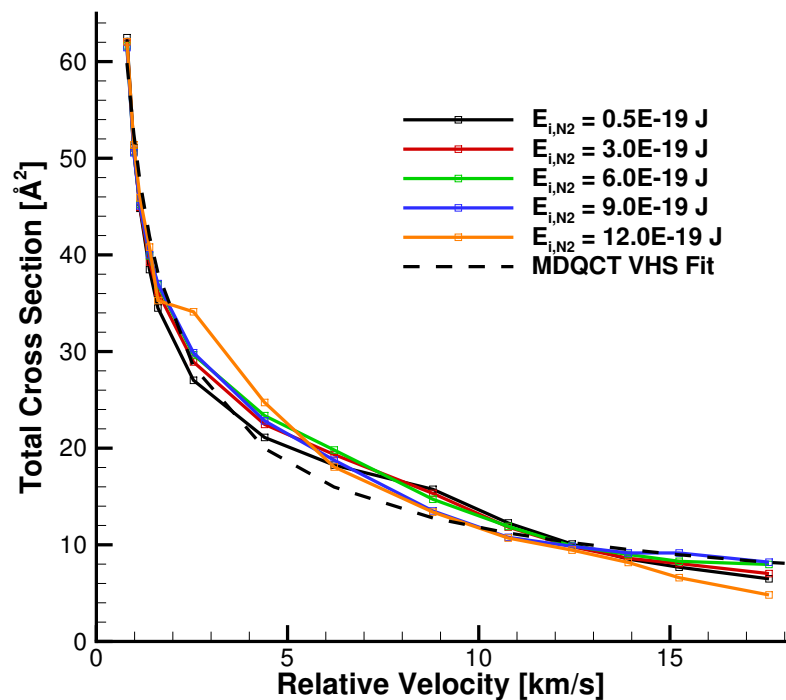
$$\sigma_{el}(T) = Q_{tr}^{-1} \sum_{E_{tr}=E_{tr,min}}^{E_{tr}=E_{tr,max}} \Delta E_{tr} \exp\left(-E_{tr}/kT\right) \sigma_{el}(T, E_{tr})$$



- $\sigma_r(T, E_{tr})$ and $\sigma_{el}(T, E_{tr})$ are averaged over rotational cross sections given as a function of J, v in Jaffe data base.
- $Z_{r,eff} \ll Z_{r,P}$,
- $Z_{r,eff}$ almost constant (1.8-3.5) almost entire temperature range.



Development of New Total Cross Section Model for N_2+N Collisions

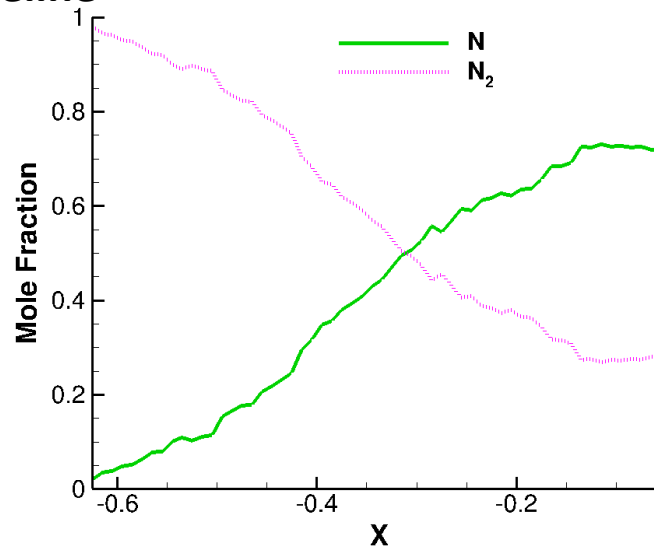
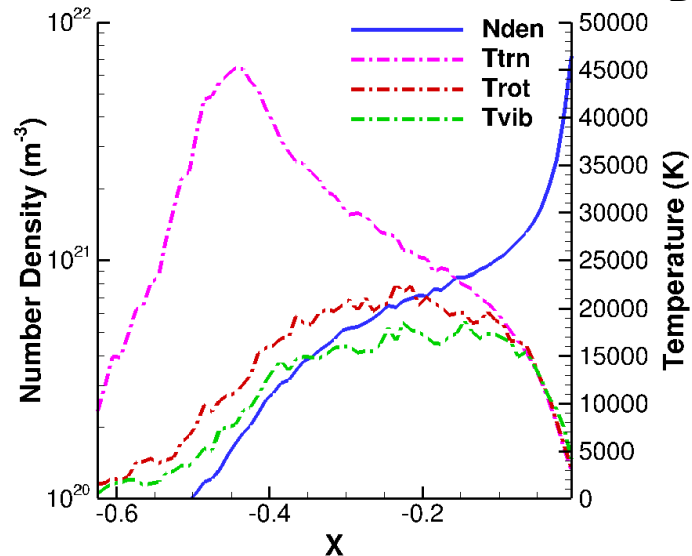


- In general, total cross section independent of internal energy.
- VHS form can still be used with MD-derived parameters.
- MD/QCT derived total cross sections > than original low-T viscosity, Bird/Ozawa values.



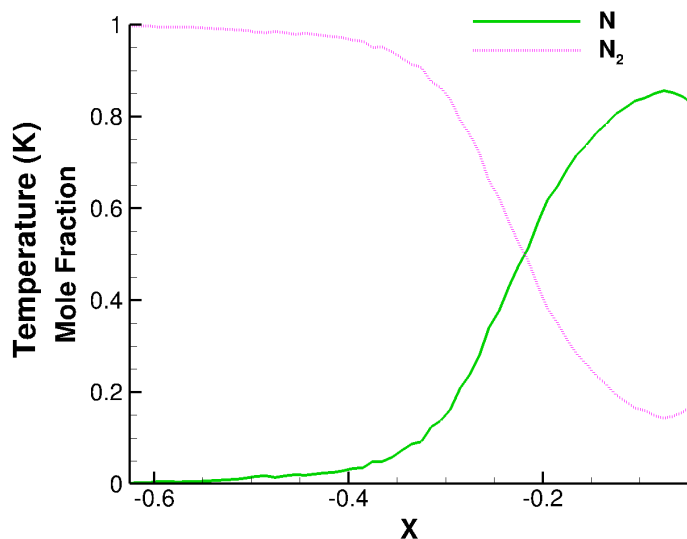
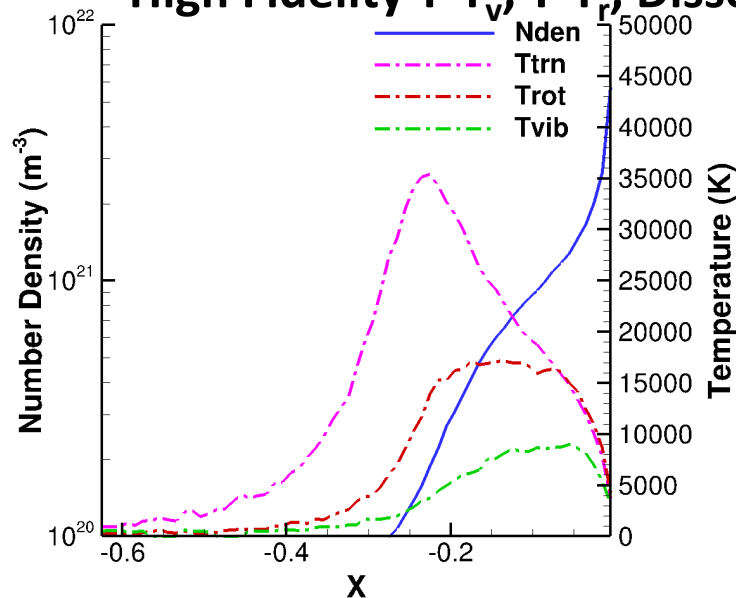
Cumulative Sensitivity of a Nonequilibrium ($Kn = 0.008$), Chemically Reacting Flow

Baseline



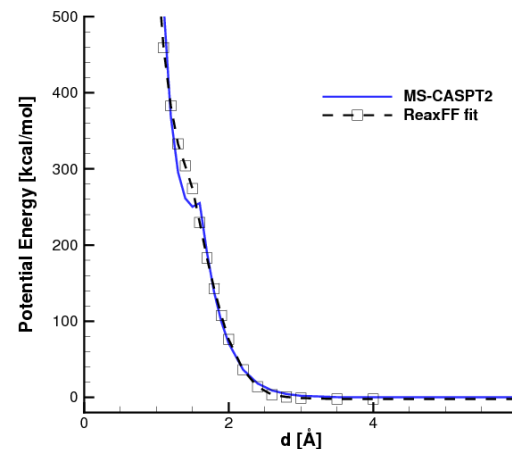
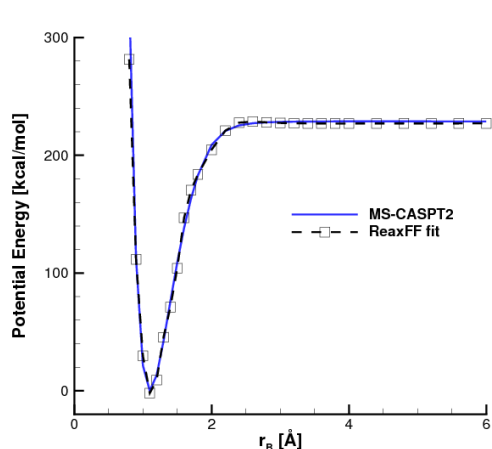
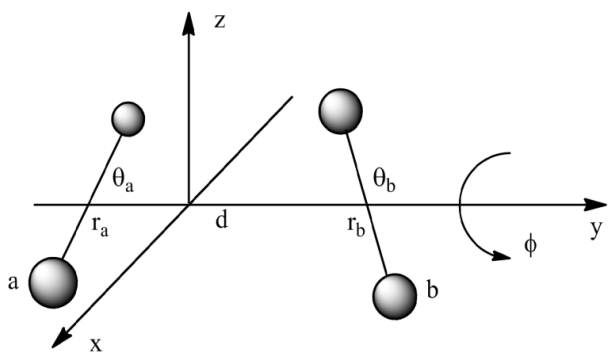
- Shock width is reduced,
- Dissociation is enhanced,
- Temperatures are decreased due to more loss of energy in dissociation reactions,

High Fidelity T-T_v, T-T_r, Dissociation, Total Cross Section



- T_{rot} more different from T_{vib} because of higher R-T rate.

Development of N₂-N₂ Potential



r_b varies, $r_a = 1.098 \text{ \AA}$, $d = 10 \text{ \AA}$, $\theta_a = 90^\circ$, $\theta_b = 90^\circ$, $\phi = 0^\circ$
 d varies, $r_a = 1.098 \text{ \AA}$, $r_b = 1.098 \text{ \AA}$, $\theta_a = 90^\circ$, $\theta_b = 90^\circ$, $\phi = 0^\circ$

- A ReaxFF form for the 4N potential is being developed using the *ab initio* computations from the University of Minnesota: over 11,000 N₂-N₂ and N₃-N geometries.
- ReaxFF potential is based on contributions from bond energies, valence and torsion angle terms, conjugation effects, and van der Waals and Coulomb interactions.
- In the fitting process, weighting can be applied to better resolve more important geometries, i.e., N₂-N₂ interactions that will lead to dissociation events in QCT trajectories.
- Less weight given to configurations corresponding to extremely high energies.



Acknowledgments

- **This research performed at the Pennsylvania State University was supported by AFOSR Grant No A001650203**